

Natural and Forced Convective Heat Transfer Enhancement for Solid Cylinders with Different Geometrical Shapes

Abid Hasan Rafi¹, Md. Rafikur Rahman¹, S. M. Fazla Rabby¹, Dewan Hasan Ahmed^{1*}

¹ Department of Mechanical and Production Engineering, Ahsanullah University of Science and Technology, 141-142 Love Road, Tejgaon Industrial Area, Dhaka 1208, Bangladesh

* Corresponding author, e-mail: dhahmed.mpe@aust.edu

Received: 17 May 2023, Accepted: 05 February 2024, Published online: 18 March 2024

Abstract

Enhancing heat transfer for both natural and forced convection is a common issue for any heat transfer process. Experimental studies have been carried out for six different geometrical shapes of solid bars for natural convection and forced convection with four different air velocities while keeping the same perimeter and length of the solid bars, which means the lateral surface area of the bars is the same. Results reveal that both the natural and forced convective heat transfer characteristics are greatly influenced by the geometrical shape in terms of Nusselt number (Nu), heat transfer coefficient (h), and heat transfer rate (q). In addition, isosceles and cylindrical shape geometry contribute to the lowest and highest heat transfer, respectively. As well, it is obtained from the results that convective heat transfer characteristics are directly related to the cross-sectional area, even if the perimeters are the same. Moreover, among the different geometrical shapes, the isosceles and hexagonal shapes take the shortest and longest duration to attain the steady-state condition in the conductive heat transfer process. The convective heat transfer characteristics are well-validated, with available results for both natural and forced convection heat transfer.

Keywords

natural convection, forced convection, geometrical shape, heat transfer, Nusselt number, heat transfer coefficient

1 Introduction

The effort to save energy and materials led to the production of more efficient heat exchangers or heat transfer equipment. Improvement in the heat transfer process, referred to as heat transfer augmentation, enhancement, or intensification, is essentially required for thermal energy systems to solve the global energy problem. This can be facilitated by enhancing the heat transfer rate by a change in size and weight of a heat exchanger, upgrading the capacity or reducing the temperature difference for the process streams, or reducing the pumping power [1]. The use of heat transfer enhancement techniques is commonly needed in process industries, refrigerators, air-conditioning equipment, power plants, automobiles, radiators for space vehicles, etc.

Heat transfer enhancement techniques can be categorized into three sections: passive, active, and a combination of both passive and active methods or compound methods. Passive techniques generally use the change of surface or geometrical modifications by including inserts or additional devices, whereas active techniques require additional power input from an outside source to achieve the desired

flow modification and improvement in the heat transfer rate. Various active and passive heat transfer enhancement techniques have been suggested to improve the internal cooling of thermal systems, such as gas turbine blades, combustor walls and electronic components, nuclear reactors, compact heat exchangers, and solar air heaters [2]. Fins [3, 4], repeated ribs [5–7], and hybrid ribs [8–10] have been used as passive heat transfer enhancements for different thermal equipment in different industrial processes.

Usually, for the study of heat transfer from a heated cylinder, the effects of conduction and radiation are considerably smaller relative to the effect of convective heat transfer [11]. In convective heat transfer, based on fluid motion, natural and forced convection are the two modes used to calculate the heat transfer rate. Natural convection takes place due to temperature differences, which affect the density as well as the relative buoyancy of the fluid, whereas forced convection, also called heat advection, occurs by fluid movement resulting from external surface forces such as a fan or pump.

Heat transfer by convection is described by Newton's law of cooling [12, 13], expressed in Eq. (1),

$$q = hA(T_w - T_\infty) \quad (1)$$

where, q = Rate of heat transfer due to convection, h = Heat transfer coefficient, A = Surface area, T_w = Wall temperature of the object, and T_∞ = Temperature of the free-stream fluid.

Convection heat transfer from a cylinder is known to be significantly affected by fluid properties such as dynamic viscosity, thermal conductivity, density, specific heat, fluid velocity, as well as geometrical factors such as size, shape, and solid surface roughness [13, 14]. Empirical correlations are available to estimate heat transfer coefficients, which are typically expressed in terms of dimensionless numbers. Those correlations are used for both natural and forced convection heat transfer calculations. Nusselt number (Nu), Reynolds number (Re), Prandtl number (Pr), Rayleigh number (Ra), and Grashof number (Gr) are commonly used to calculate heat transfer performances. Nusselt number (Nu) is the ratio between convective and conductive heat transfer. Reynolds number (Re) is the ratio of inertia force and viscous force. Prandtl number (Pr) depicts the ratio between viscous and thermal diffusion rates since it represents the ratio between kinematic viscosity and thermal diffusivity. The onset of natural convection can be determined by the Rayleigh number (Ra). The product of the Grashof number (Gr) and the Prandtl number (Pr) is called the Rayleigh number (Ra). The definitions of Nusselt number (Nu), Reynolds number (Re), Prandtl number (Pr), Grashof number (Gr), and Rayleigh number (Ra) are expressed in Eqs. (2)–(6).

$$\text{Nu} = \frac{hd}{k} \quad (2)$$

$$\text{Re} = \frac{\rho u_\infty L}{\mu} \quad (3)$$

$$\text{Pr} = \frac{\vartheta}{\alpha} = \frac{C_p \mu}{k} \quad (4)$$

$$\text{Gr} = \frac{g\beta(T_w - T_\infty)L^3}{\nu} \quad (5)$$

$$\text{Ra} = \text{Gr} \cdot \text{Pr} \quad (6)$$

where, d = hydraulic diameter; k = thermal conductivity; ρ = density; u_∞ = the velocity of the freestream fluid; L = characteristic length; μ = dynamic viscosity; ϑ = Momentum diffusivity; α = thermal diffusivity; C_p = Specific heat; g = Gravitational acceleration; β = Thermal expansion coefficient; ν = Kinematic viscosity.

Fins have always been used as a passive method of enhancing the convective heat transfer from cylinders [15, 16]. This technique is widely used in applications, such as power stations, cooling engines, cooling systems, vapor cooling systems, etc. Therefore, optimization of the fin design is very important to reduce the size of the heat transfer equipment and, consequently, to use less material. Using fins increases the heat transfer area, which causes an increase in the quantity of transferred heat, but they also increase the turbulence of the flowing fluid [17].

The existence of solid fins has an impact on the aerodynamic and thermal characteristics of the flow [18]. As a result of the differential heating of fluid around the fin surfaces, heat transfer occurs across the thermal boundary layer [19]. The heat transfer from rectangular arrays of straight fins on a horizontal surface in natural convection, as well as the forced convection heat transfer on these fins, has been widely investigated in the literature [20–24]. Adhikari et al. [25] presented an experimental and numerical study of forced convection heat transfer from straight rectangular fins on a horizontal surface at low Reynolds numbers ranging from 2600 to 6800, which revealed that forced convection heat transfer is characterized by a nearly linear relationship between Nusselt number and Reynolds number, which is also matched with the existing correlations for fully developed turbulent convective heat transfer reasonably well. Kaddle and Sparrow [23] investigated the fully developed heat transfer from shrouded fin tips for turbulent airflow analytically, experimentally, and numerically for $5.000 < \text{Re} < 35.000$. And their conclusions for the average Nu matched those for fully formed circular tube flow. Chen et al. [26] used the inverse approach to compute the heat transfer coefficient of a rectangular heat sink with different fin spacing. Sun et al. [27] investigated heat transfer from rectangular channels using water as the fluid under uniform and non-uniform heating and derived correlations for laminar and transition regions up to $\text{Re} = 10.000$.

Bilen et al. [16] studied heat transfer from a surface with cylindrical fins and found that heat transfer increased as Re increased; however, heat transfer enhancement declined as Re increased. Therefore, the staggered arrangement of the fins produced a slightly higher enhancement than the in-line configuration. VanFossen [28] compared the overall heat transfer coefficients in rectangular ducts with staggered arrays of short and long pin fins in experimental research. The results showed that short pin fins performed better than long pin fins in terms of overall heat transfer.

An extensive investigation can be found on heat transmission for a geometrical shape of a circular cylinder with a wide range of Nusselt numbers and Reynolds numbers [29–31]. Nakamura and Igarashi [30] measured the heat transfer in the separated flow behind a circular cylinder, ranging from $Re = 70$ to $30,000$, which covered the laminar shedding, the wake transition, and the shear-layer transition regimes. The results of Richardson [32] and Igarashi and Hirata [33] are consistent with Nakamura and Igarashi [30] for the higher Reynolds numbers ($Re > 1.5 \times 10^4$). Hilpert [31] also investigated heat transfer from a circular cylinder over a large range of Reynolds numbers, from 2×10^5 to 2.3×10^5 , and reported an empirical relationship between the Reynolds number and the overall Nusselt number. At $Re = 4, 40, 4,000, \text{ and } 40,000$, he discovered the discontinuities in the slope of the correlation, which he believes are due to the changes in the flow pattern. Therefore, it is important to establish a relationship between the flow and the fin geometrical characteristics to maximize heat transfer both in natural and forced convection while using the least amount of fan or pump power possible.

Many analytical, numerical, and experimental studies have been conducted to clarify the impact of confinement on natural convection heat transfer performance from horizontal, heated cylinders immersed in a fluid and developed a correlation equation for the mean value of Nu over the cylinder for a wide range of Rayleigh number, Ra and Prandtl number, Pr [29, 34–39]. A set of empirical correlation equations for the prediction of Nu for Rayleigh number range $3.6 \times 10^4 < Ra < 9.2 \times 10^5$ and Prandtl number range $4.5 \leq Pr \leq 160$ has been developed [34]. Following the model proposed by Churchill and Usagi [40], Churchill and Chu [41] developed one of the most famous correlation equations for the mean value of Nu over the cylinder for all Ra numbers and all Pr numbers.

An empirical correlation is proposed by Morgan [29] for the full range of Rayleigh numbers, while Kuehn and Goldstein [35] proposed an analytically based correlation for natural convection heat transfer from a horizontal cylinder that is valid at any Rayleigh and Prandtl number. According to Kuehn and Goldstein [36], if the outer border is not positioned far enough from the cylinder's surface, it affects the calculated values of the heat transfer coefficient. Rath et al. [39] investigated natural convection from horizontal cylinders of various shapes in a rectangular cavity (57×30 mm) in the laminar regime with a Rayleigh number in the range of $10^3 \leq Ra \leq 10^6$. It is shown that the Nusselt numbers are substantially influenced by

the cylinder's form. The Nu of a circular cylinder is significantly greater than that of a triangular or square cylinder with the same surface area.

Many researchers worked to observe the effect of changing the shape of the rib [42–45]. According to the authors, the effect of rib form on the heat transfer coefficient vanishes at higher Reynolds numbers. The triangular-shaped rib has the maximum heat transfer coefficient among square, triangular, circular, and semi-circular ribs [42]. On the other hand, Wang and Sundén [43] show that the trapezoidal-shaped ribs achieve the highest heat transfer enhancement factor as a result of an experiment in a square duct roughened with square, equilateral-triangular, trapezoidal ribs. In addition to experimental investigations, several computational studies have also been carried out to investigate the effect of rib shapes on flow structures and heat transfer patterns for ribbed ducts. Large-eddy simulations are performed by Vázquez et al. [46] to investigate the effect of several types of ridges, such as circular, triangular, and trapezoidal, on heat transfer characteristics in a square duct flow. It is shown from the study that the trapezoidal-ridged duct induces a 200 percent increase in turbulent heat flux when compared with a square duct.

Promvong and Thianpong [47] studied the thermal performance assessment of forced convection heat transfer for airflow inside the channel with different shaped ribs. In that particular study, the rib cross-sections are triangular (isosceles), wedge (right triangular), and rectangular shapes for Reynolds numbers range of $4,000$ to $16,000$ in a rectangular channel. The wedge rib increases the Nusselt number and friction factor the most, but the triangular rib with a staggering array surpasses the others in terms of thermal performance. A close examination reveals that all the wedge and triangular ribs yield higher heat transfer than the rectangular one for all Reynolds number values, similar to the result of Ahn [42].

The major objective of the present study is to investigate the heat transfer for different geometrical shapes while keeping the same perimeter. The studies have been conducted for both natural and forced convective heat transfer in a square duct. In addition, different empirical heat transfer equations are considered to calculate the Nusselt number and the related heat transfer characteristics.

2 Experimental setup and methodology

An experimental setup with a full length of $2,133.6$ mm is used in the present study. Figs. 1 and 2 represent the front view of the setup with dimensions and the section

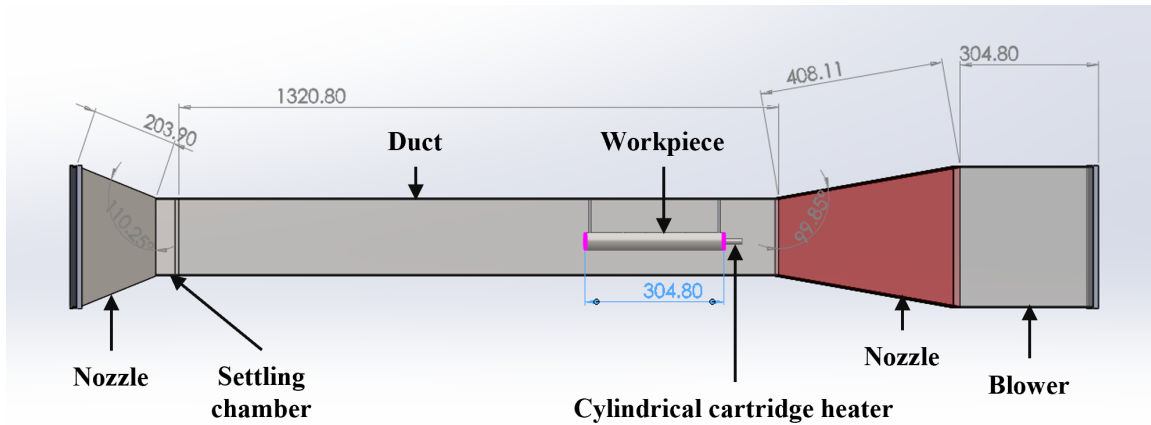


Fig. 1 Front view of experimental set up with dimensions (All dimensions are in mm)

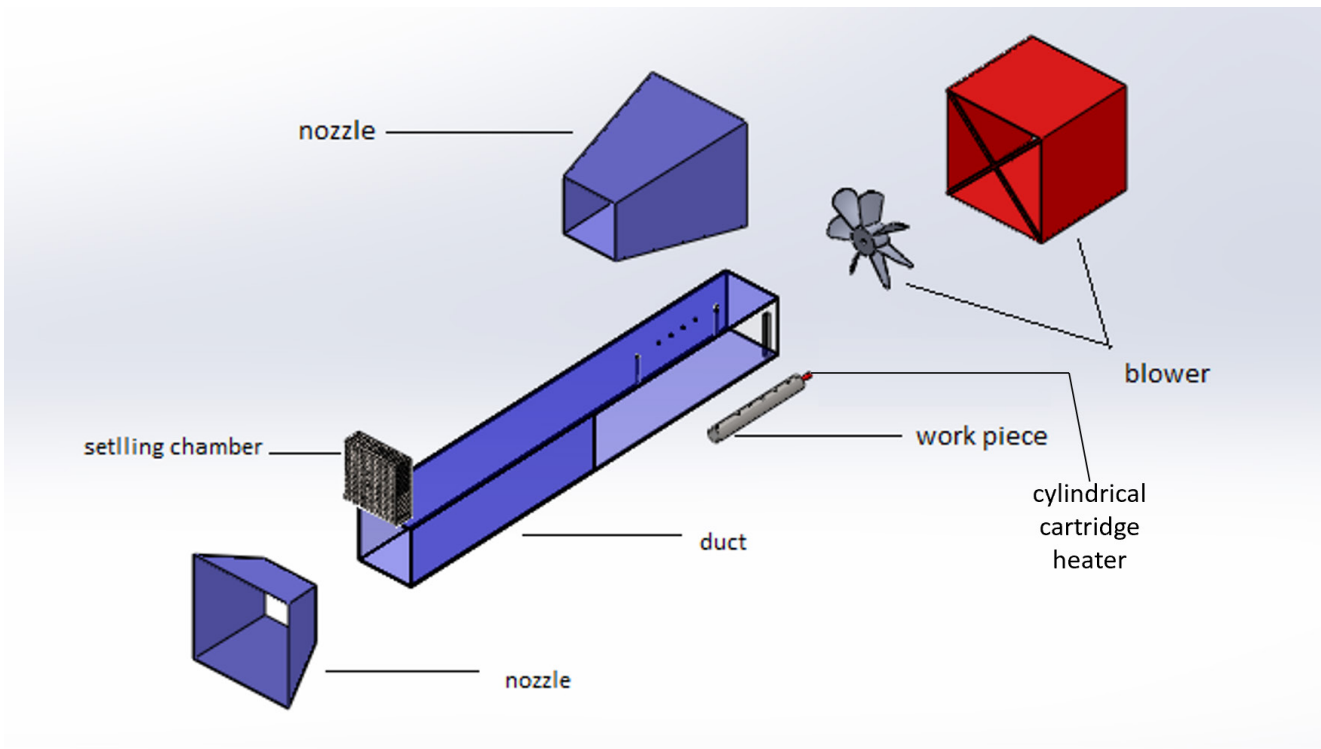


Fig. 2 Section view of experimental setup

view of the setup, respectively. The experimental setup is mainly consisting of a blower, a nozzle, and a diffuser with different lengths and selective angles, a square duct with a settling chamber, a heater, and a test section where the workpiece can be placed with the availability to attach five thermocouples in a specific distance of interval.

The diameter of the blower is 254 mm, and the length is 382 mm which is connected to a dimmer to control the air flow rate. The experimental studies are conducted with four different air velocities, i.e., 2 m/s, 4 m/s, 6 m/s, and 8 m/s by controlling the blower speed. A pitot tube anemometer (DT-8920) is used to measure the velocity of the air at the upstream position of the specimen or the solid

bar inside the duct. In this experiment, a single heating coil of 400 Watt, and 220 volts has been used, which is a cylindrical shape with a diameter of 10 mm and a length of 100 mm. The mild steel solid bar specimens of different shapes are drilled with a 9.5 mm diameter with a length of 100 mm at one end along the length at the trailing end of the bar, and the heating coil is well inserted into the specimen. The detailed specifications of the instrument used during the experimental study are given in Table 1.

The diffuser has a relatively longer length of 408.11 mm and the angle is 9.85° whereas the length of the nozzle is 203.90 mm and the angle is 20.25° . The settling chamber (circular mesh structure) serves to maintain a calm flow

Table 1 Specifications of different instruments used during the experiments

Equipment/Instrument	Specifications
Heater	Type: Cylinder type Capacity: 400 Watt Length: 10 cm Diameter: 1.0 cm Material: Mild Steel
Blower	Type: Portable Axial Blower Power: 320 Watt Maximum Speed: 2800 rpm Maximum Voltage: 220 Volt Diameter: 25 cm
Thermocouple	Type: K type Temperature Range: 3.000 °C
Temperature Display Meter	Type: K type Temperature Range: 399 °C
Blower Dimmer	Maximum Voltage: 250 Volt
Anemometer	Model: CEM DT-8920 Range: 1 to 80.00 m/s Resolution: 0.01 Accuracy: ±2.5% of reading at 10 m/s

by suppressing irregularities such as swirl, low-frequency pulsation, and turbulence. The settling chamber has a length of 127 mm and height × width of 127 × 127 mm². The test section has a length of 1320.8 mm and the cross-section (height × width) is 127 × 127 mm².

Fig. 3 shows the overall experimental setup, an induced blower is placed at the one end of the duct which sucks natural air as a working fluid and finally exits as hotter air. In this investigation, five thermocouples have been used to find out the heat transfer values of five points in the experimental specimen bar. All the thermocouples that have been used are K-type. In addition, five individual displays have been used to observe the temperature of different thermocouples for necessary data collection.

The cross-sectional view of the six different geometrical shapes solid bar for the experimental studies is shown in Fig. 4. The different geometrical shapes of the solid bars are square, circular, equilateral, isosceles, hexagonal, and trapezoidal.



Fig. 3 Experimental setup during operation

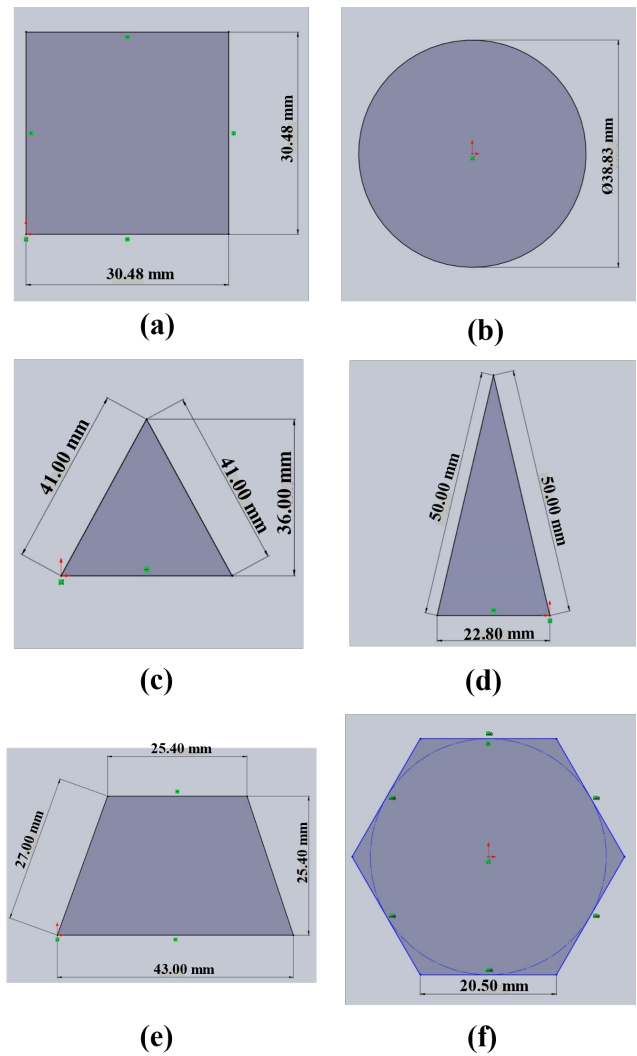


Fig. 4 Cross-sectional view of different geometrical shapes (a) square, (b) cylindrical, (c) equilateral, (d) isosceles, (e) trapezoidal, and (f) hexagonal

These bars are 12 inches each or 0.3048 m in length and have the same perimeter of 0.122 m which means the lateral surface area over the length is the same which is 0.037 m². Each bar has five holes on the surface which are drilled to the center of the bar to attach thermocouples that are staying on the top of the bar. The bar is hung in such a way that the centerline of the bar and the duct are inline. After hanging the bar, the cover is placed as shown in Fig. 3. The temperature at different points along the bar can be obtained from the thermocouples. The samples of the bars for the experimental studies are shown in Fig. 5.

3 Data processing

The convective heat transfer parameters are calculated from the collected data during the heating and cooling operations on six different geometrical shaped solid bars with different

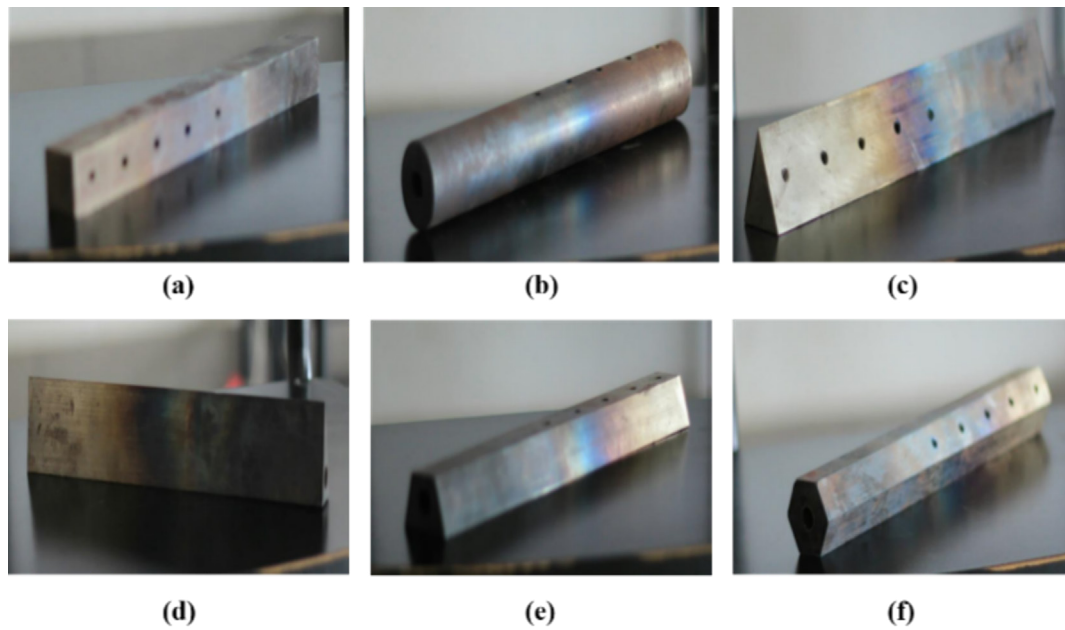


Fig. 5 Solid bars with different geometrical shapes (a) square, (b) cylindrical, (c) equilateral, (d) isosceles, (e) trapezoidal, and (f) hexagonal

cooling conditions. The wall temperature, T_w in Eq. (1) has been determined by averaging the wall temperature collected from thermocouples placed in 5 different positions.

All of the bars are heated over $150\text{ }^\circ\text{C}$ and ensure a steady state condition for at least 2–3 minutes and then cooled down by both natural and forced cooling. For forced cooling, fluid flow is generated by using the blower with velocities of 2 m/s, 4 m/s, 6 m/s, and 8 m/s. It should be mentioned here that the thermocouple T1 is positioned closest to the heater, which is the far downstream position of the solid bar with respect to the fluid flow direction. On the other hand, the thermocouple T5 is at the farthest distance from the heater, i.e., at the upstream position.

At first, the solid bars are heated without the presence of any external fluid flow until the temperature on the solid surface reaches a steady state. Fig. 6 shows the temperature increase trend for different geometrical shaped solid bars. It is quite interesting that the time required to reach the steady state for the temperature differs for the different geometrical solid bars. It is evident from the Fig. 6 that the isosceles solid bar takes a shorter time while the hexagonal solid bar takes a longer time to reach a steady state in temperature. It should be noted here that the steady state is considered when the temperature readings of the thermocouples are stable for around 2–3 minutes. Therefore, it will be quite interesting how the solid bars with different geometrical shapes act on heat transfer issues.

Once the steady state is attained for the heating of the solid bars, the heater is turned off, allowing the heated

metal bars to cool down through natural convection. The temperature decreasing trends to reach the steady state are shown in Fig. 7. It should be mentioned that the temperature decreasing trends for all the geometrical shapes of the solid bars are similar to natural cooling. However, the conductive heat transfer through the metal bar is still active as T5 decreases at a slower rate for the first few minutes. Anyway, it is evident from the Fig. 7 that the isosceles bar is cooled over the shortest period of time, and the hexagonal shape takes the longest period of time.

Having a closer look at the temperature increasing and decreasing graphs, some interesting issues are obtained. For example, temperature rises from ambient temperature (which is around $25\text{ }^\circ\text{C}$) to $250\text{ }^\circ\text{C}$ for all the solid bars (consider the thermocouple 1, which is closed to the heater), the cylindrical bar takes much less time (around 29 minutes), while the equilateral bar takes around 41 minutes. However, isosceles and hexagonal bars take around 37 and 39 minutes, respectively, as shown in Fig. 8. This might be the reason that during the heating of the solid bars, the natural convection is also taken place. Therefore, once the heater is turned on, the natural convection also takes place. Therefore, in the natural cooling process (from $250\text{ }^\circ\text{C}$ to $70\text{ }^\circ\text{C}$) isosceles takes the lowest time around 38 minutes whereas hexagonal takes the longest time around 70 minutes. However, cylindrical and equilateral bars take around 62 and 49 minutes, respectively. Therefore, it is interesting how the natural heat transfer takes place for solid bars with different geometrical shapes.

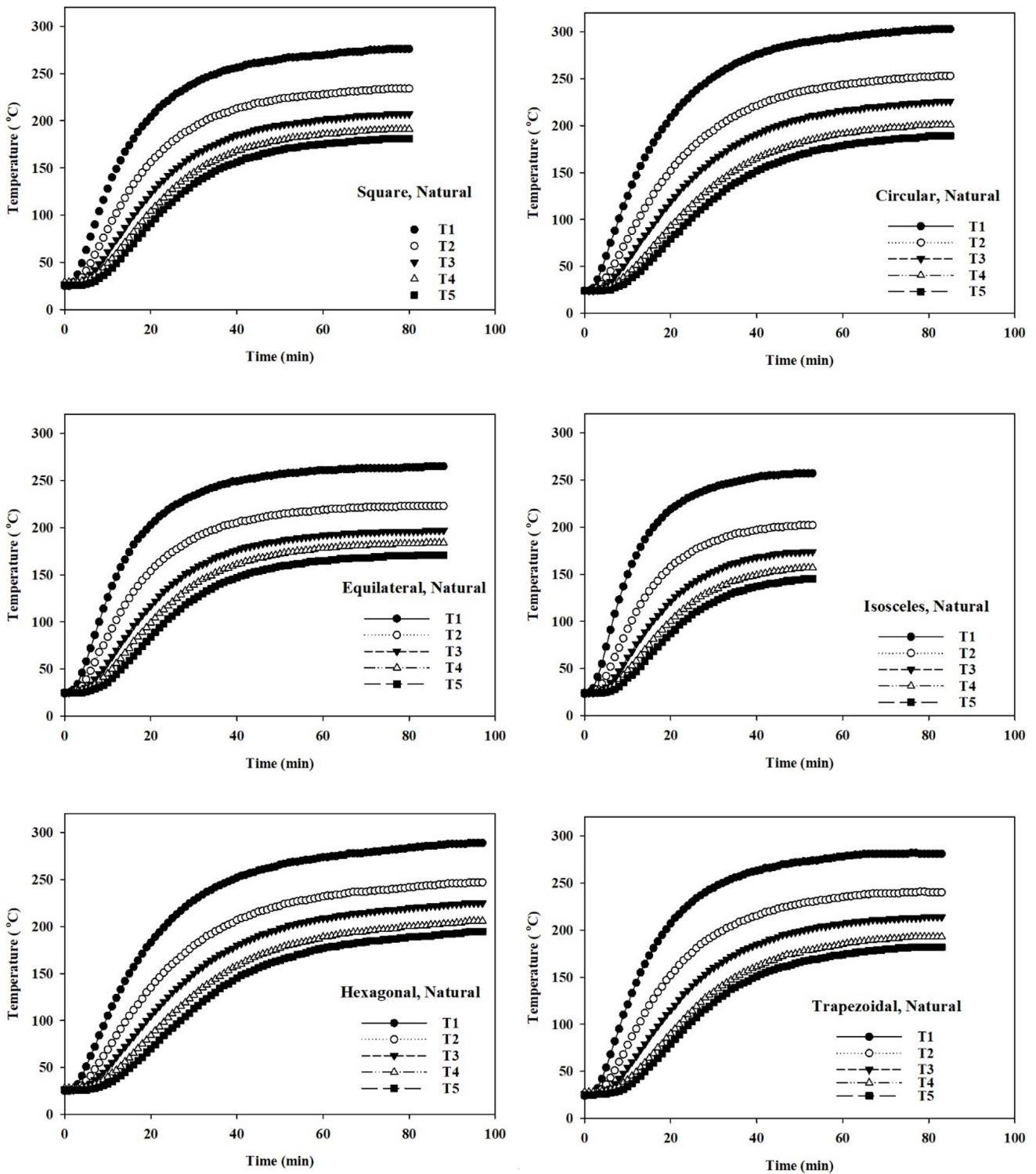


Fig. 6 Time history to attain a steady state in temperature for different geometrical shape solid bar during heating

The experimental study is continued for the forced convective heat transfer by maintaining the same procedure as the solid bars are heated first until a steady state is achieved, and the heater is turned off and the blower is turned on. The experiments are repeated for 4 different air velocities

(i.e., 2, 4, 6, and 8 m/s). It should be mentioned here that the temperature increasing profile for all the bars has a similar pattern as described in Fig. 6. Therefore, the temperature decreasing profiles of the isosceles and hexagonal bars for the forced convective heat transfer case are shown in Fig. 9.

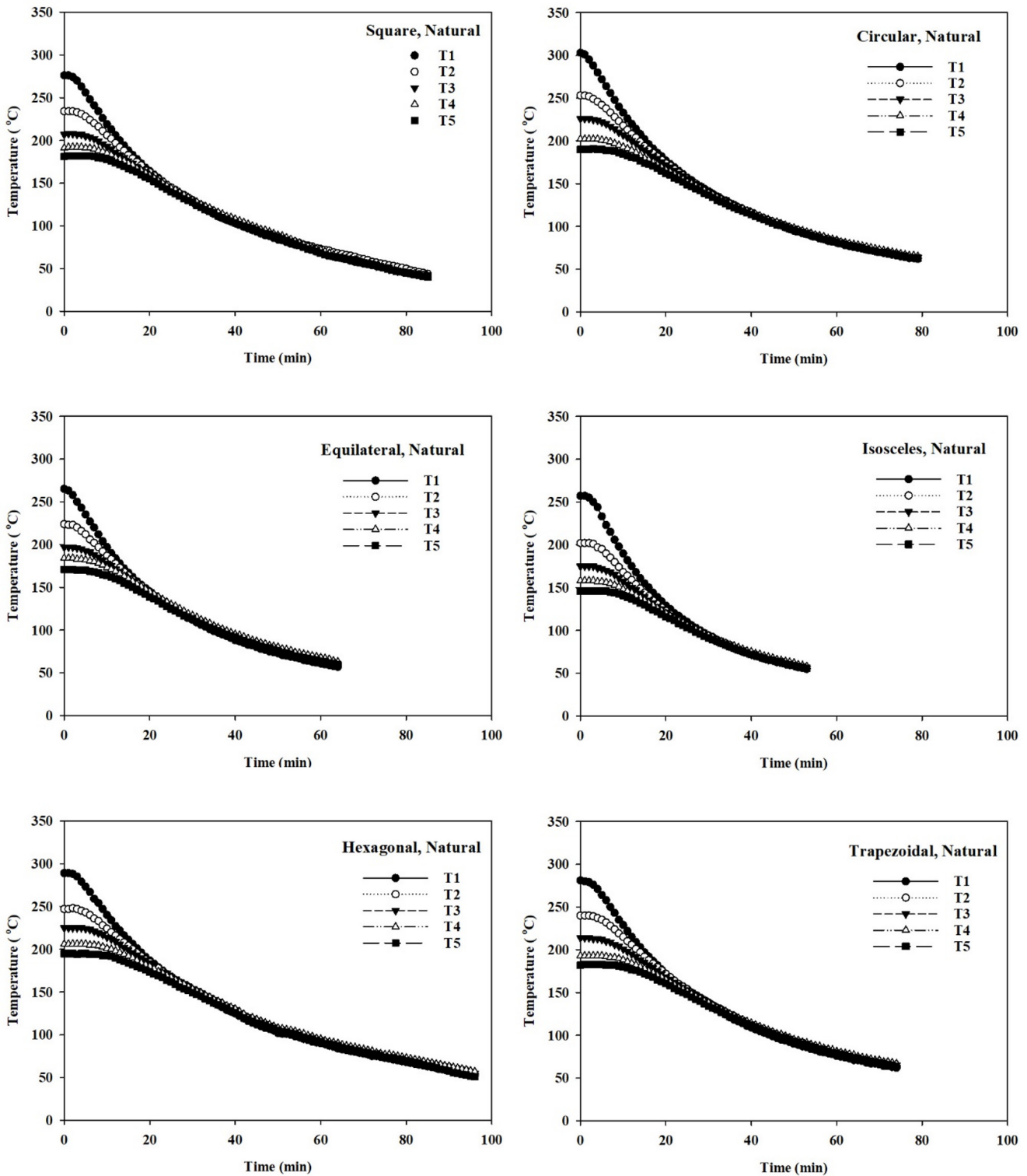


Fig. 7 Time history to attain a steady state in temperature for different geometrical shape solid bar during natural cooling

It is clearly observed that the temperature drops much quicker for the isosceles bar as compared with the hexagonal bar. Moreover, the temperature decreasing trend is much faster in forced cooling than that of natural cooling

specially at the earlier stage of the cooling process. In fact, for the natural convection, the temperature maintains the initial temperature for a while and then starts decreasing at a slower rate however, the temperature drops very sharply

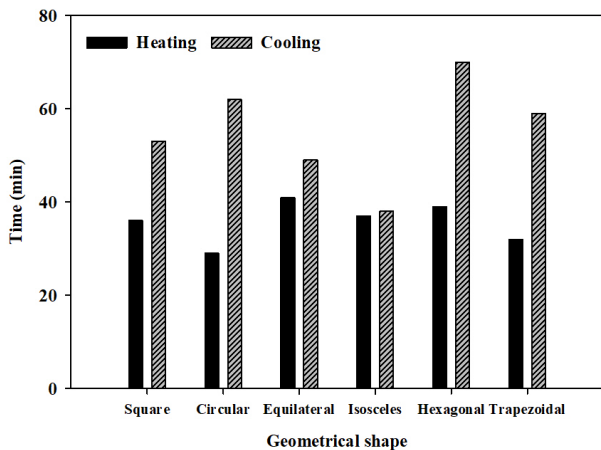


Fig. 8 Duration of time during the heating and cooling of the solid bar. Heating is considered from 25 °C to 250 °C and cooling is considered from 250 °C to 70 °C.

at the beginning of the cooling process and it is much more intense for the higher air velocities. However, increasing the air velocity enhances the heat transfer for all cases.

Based on the temperature profiles for the cooling processes the respective heat transfer characteristics for both the natural and forced convection are explained in the following sections.

3.1 Empirical relations for natural convection

From the study of many researchers [29, 40, 41, 48] it is found that the average natural convective heat transfer coefficients can be represented in the following function of Nu for a variety of circumstances shown in Eq. (7),

$$Nu = C(Gr \cdot Pr)^m, \quad (7)$$

where the properties of the dimensionless groups are evaluated at the film temperature, T_f which is the arithmetic mean of free-stream temperature, T_∞ , and wall temperature of the object, T_w . For the values of the constants, C and m , the predictions of Morgan [29] are the most reliable and are presented in Table 2.

A more complicated but very effective expression for use over a wider range of $Gr \cdot Pr$ ($10^{-5} < Gr \cdot Pr < 10^{12}$) is given by Churchill and Chu [41] as shown in Eq. (8),

$$Nu^{1/2} = 0.60 + 0.387 \left(\frac{Gr \cdot Pr}{\left(1 + (0.559 / Pr)^{16/9}\right)^{1/4}} \right)^{1/6}. \quad (8)$$

The value of Nusselt number, Nu calculated by using Eq. (7) for natural convection is denoted as Nu_1 whereas the value extracted by using Eq. (8) is denoted as Nu_2 .

3.2 Empirical relations for forced convection heat transfer

For higher Reynolds numbers, the heat transfer is predominated by forced convection. Knudsen and Katz [48] is suggested the following correlation for Nusselt number as shown in Eq. (9),

$$Nu = C \left(\frac{u_\infty d}{\nu} \right)^n Pr^{1/3}. \quad (9)$$

The values for C and n are provided in Table 3.

A more comprehensive relation is given by Churchill and Bernstein [49] which is applicable over the complete range of available data (for $10^2 < Re < 10^7$ and $Pr > 0.2$) shown in Eq. (10),

$$Nu = 0.3 + \frac{0.62 Re^{1/2} Pr^{1/3}}{\left[1 + \left(\frac{0.4}{Pr}\right)^{2/3}\right]^{1/4}} \left[1 + \left(\frac{Re}{282000}\right)^{5/8}\right]^{4/5}. \quad (10)$$

The value of Nusselt number, Nu is calculated by using Eq. (9) for forced convection is denoted as Nu_1 whereas the value extracted by using Eq. (10) is denoted as Nu_2 .

4 Results and discussion

4.1 Natural convection result analysis

In this present study, the heat transfer parameters due to natural or free convection are studied for different geometrical shapes with the same perimeter for the purpose of finding out the most effective geometrical shapes in terms of convective heat transfer. Circular cylindrical shape geometry is the most common for heat transfer calculation and can be found in literature [29, 35, 36]. Nusselt number, Nu and Rayleigh number, Ra are mostly used dimensionless numbers for natural convective heat transfer study.

The values of the Nu of the circular cylinder are extracted from the present study for different Rayleigh number, Ra and compared with the result with the literature [29, 36] as shown in Fig. 10 (a). The data obtained from the present study are perfectly fitted with the previous literature while supporting the trend.

The Nusselt number, Nu_1 , and Nu_2 with respect to Rayleigh number, Ra calculated by using Eqs. (7) and (8) respectively for different geometrical shapes are presented in Fig. 10 (b). It is visible from the Fig. 10 (b) that the Nusselt number (Nu) has a rising tendency with the increase of Rayleigh number, Ra for natural convective heat transfer.

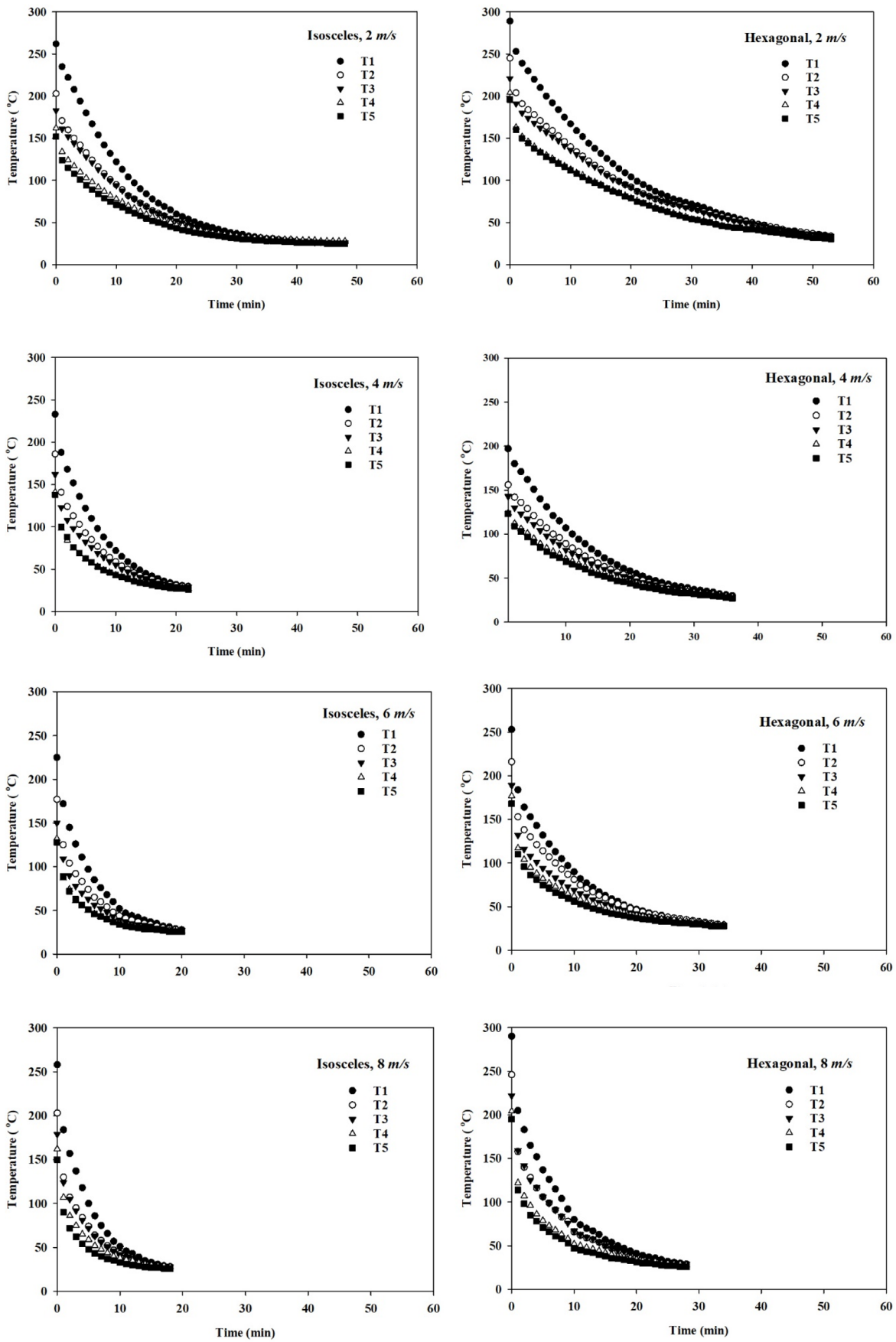


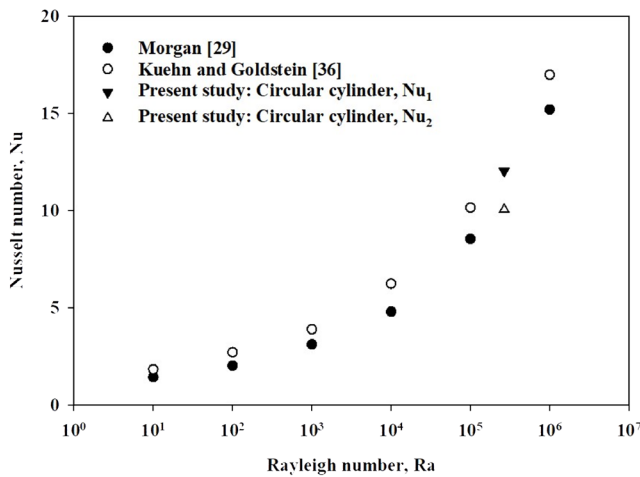
Fig. 9 Time history to attain a steady state in temperature for isosceles and hexagonal geometrical shape solid bar during forced cooling

Table 2 Table provided by Morgan [29] for natural convection

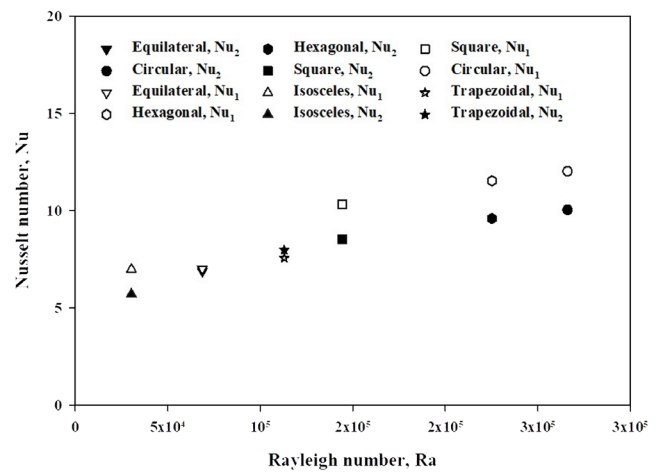
Ra = Gr·Pr	Nu = C (Gr·Pr) ^m	
Range	C	m
10 ⁻¹⁰ to 10 ⁻²	0.675	0.058
10 ⁻² to 10 ²	1.02	0.148
10 ² to 10 ⁴	0.850	0.188
10 ⁴ to 10 ⁷	0.480	0.250
10 ⁷ to 10 ¹²	0.125	0.333

Table 3 Table provided by Knudsen and Katz [48] for forced convection

Re	C	n
0.4–4	0.989	0.330
4–40	0.911	0.385
40–4,000	0.683	0.466
4,000–40,000	0.193	0.618
40,000–400,000	0.0266	0.805



(a)



(b)

Fig. 10 Natural convective heat transfer in Nu-Ra map (a) performance of circular shape compared with the available literature, (b) comparison between six different geometrical shapes conducted in the present study

According to the literature, the Nusselt numbers are substantially influenced by the cylinder's form. The Nu for a circular cylinder is significantly greater than that of a triangular or square cylinder with the same surface area [39]. In the present study, the isosceles shape shows a lower value of the Nusselt number as well as a lower Rayleigh number. While the circular and hexagonal shapes possess a higher value of Nu and Ra during the natural cooling. In fact, for the circular shape, the Nu is a little higher than the hexagonal shape, thereby aligning with established findings in the literature.

The heat transfer coefficient, h (W/m² °C), and heat transfer rate, q (W) are also calculated in this study of natural convection for different geometrical shapes and Nusselt numbers, Nu₁, and Nu₂ using Eqs. (1) and (2) as shown in Fig. 11. The heat transfer coefficient, h_1 (W/m² °C), and heat transfer rate, q_1 (W) have been obtained from Nu₁ and similarly h_2 and q_2 have been obtained from Nu₂. From Fig. 11 (a), it is visible that the heat transfer coefficient for different geometries stays in very close range with each other. Among those, the isosceles one has a higher value of h whereas the trapezoidal one has a lower value of h .

The square, circular, and hexagonal shapes have very similar values of heat transfer coefficient. The heat transfer rate, q (W) for different geometrical shapes during natural convection is shown in Fig. 11 (b). The isosceles shape has the minimum value of q for the same perimeter whereas the circular shape has the highest value of q in the same condition. In addition, the hexagonal exhibits second highest, and the equilateral shows the second lowest heat transfer rate.

4.2 Forced convection result analysis

Experimental studies are continued to investigate the forced convective heat transfer for geometrical shapes of the solid bars for four different air velocities in the range of 2 to 8 m/s.

There are a number of studies in the literature to obtain Nusselt numbers for a wide range of Reynolds numbers [16, 30, 31, 49]. The results extracted from the present study for the circular cylinder and compared with the available literature as shown in Fig. 12 (a) [16, 30, 31, 50–52]. The result collected from the present study shows a similar trend and well validated with the previous studies. Fig. 12 (b) depicts the value of Nu for different geometrical

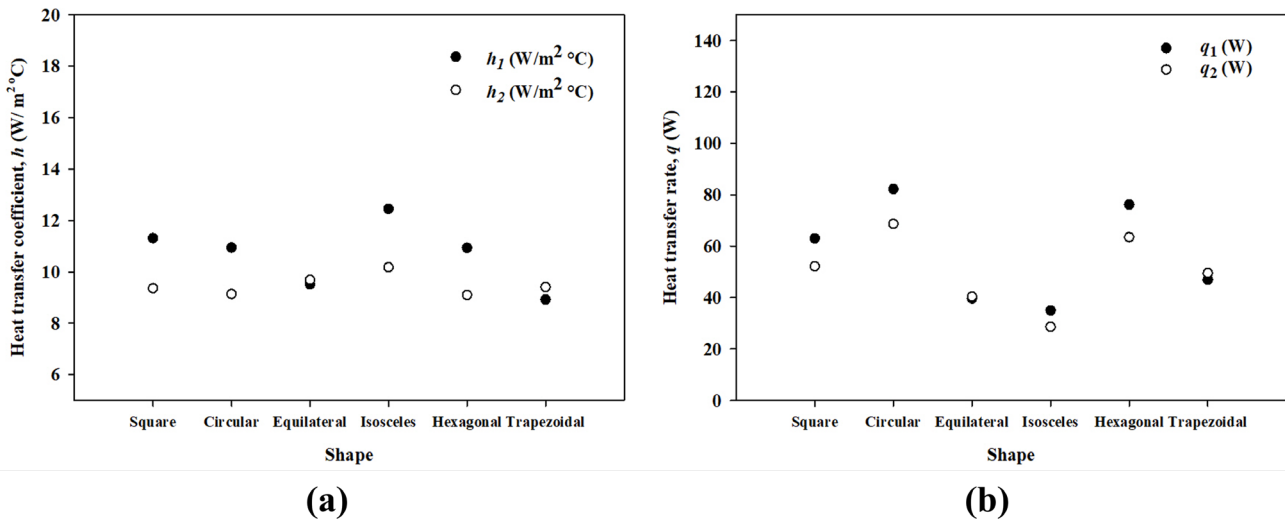


Fig. 11 Natural convective heat transfer performance of different geometrical shapes (a) heat transfer coefficient, h ($W/m^2 \text{ } ^\circ C$), (b) heat transfer rate, q (W)

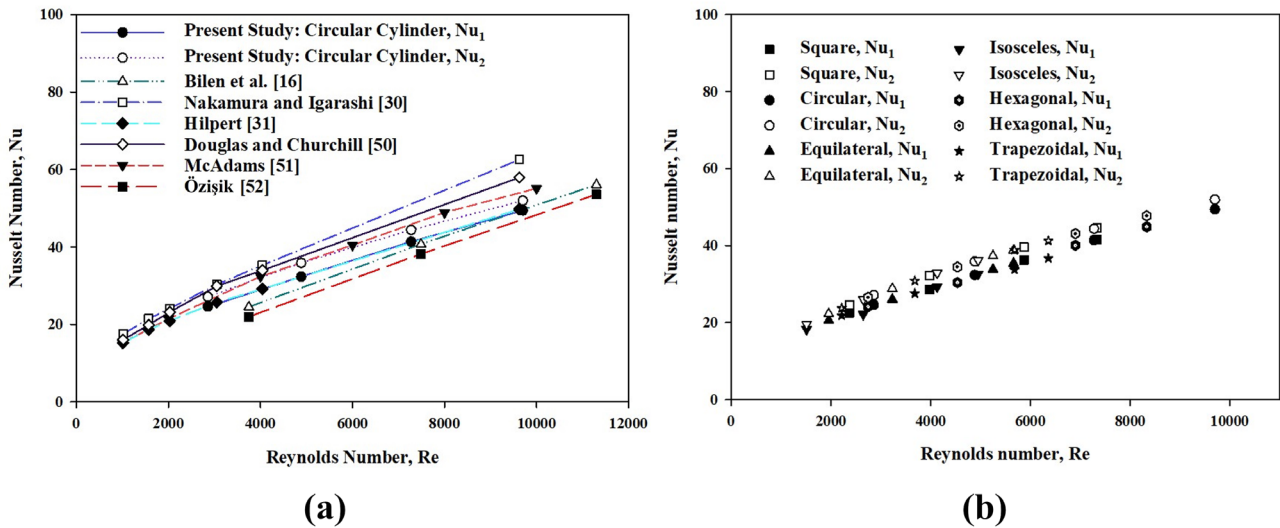


Fig. 12 Forced convective heat transfer in Nu-Re map (a) performance of circular shape compared with the available literature [16, 30, 31, 50–52], (b) comparison between six different geometrical shapes conducted in the present study

shapes in a graph of Nu-Re. The Nu_1 and Nu_2 are calculated for forced convection by using Eqs. (9) and (10) respectively. From Fig. 12 (b), it is shown that the Nusselt number is increasing with the increment of Re for all the geometrical shapes.

The trend of Nu with the variation of the Re for different geometrical shapes obtained in Fig. 12 (b) can be expressed as an equation similar to Eq. (11).

$$Nu = a Re^b \tag{11}$$

Based on the experimental results over the range of Re (1.500 to 9.300), the calculated Nu (by using Eqs. (9) and (10)) are plotted for each geometrical shape in a graph and with the best fit power law. The values for a , and b based on the present experimental study for different

geometries are provided in Table 4. Therefore, the values of a and b given in Table 4, could be useful to calculate necessary heat transfer characteristics for a given geometrical shape. Nakamura and Igarashi [30] proposed the values of $a = 0.21$ and $b = 0.62$ for the range of $2.000 < Re < 20.000$

Table 4 The value of a and b for Nu-Re correlation in convective heat transfer

Shape	$Nu = a Re^b$	
	a	b
Square	0.3696	0.5335
Circular	0.3187	0.5514
Equilateral	0.4289	0.5155
Isosceles	0.4584	0.506
Hexagonal	0.331	0.5465

as they investigated the correlation between the overall Nusselt number and the Reynolds number for cross-flow past a circular cylinder. In the context of the power law, the circular cylinder exhibits the lowest value of a compared to other geometrical shapes.

Fig. 13 presents more enormously the change of Nu for different geometrical shapes. The variations of the Nu among the geometrical shapes are less in the natural flow velocity of the air and the variations are increasing more and more with the increase of air velocity. The isosceles shape shows the minimum value of Nu compared to the values of Nu for the other shapes. In the present study, the value of Nu for the highest air velocity has been found in circular shapes.

Likewise, in the natural convective heat transfer study, the heat transfer coefficient, h ($W/m^2 \text{ } ^\circ C$), and heat transfer rate, q (W), are also studied for different geometrical shapes with multiple air velocities.

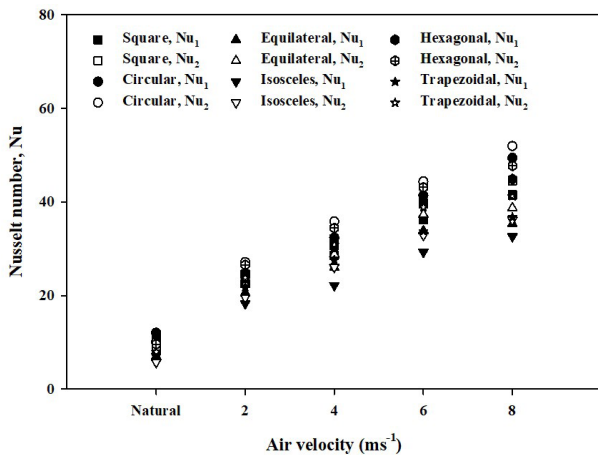
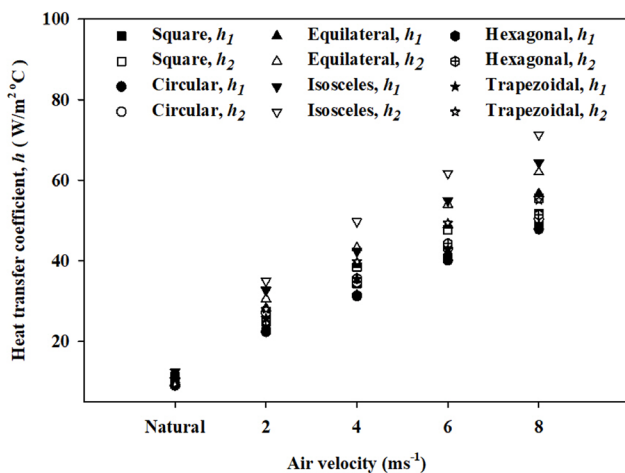
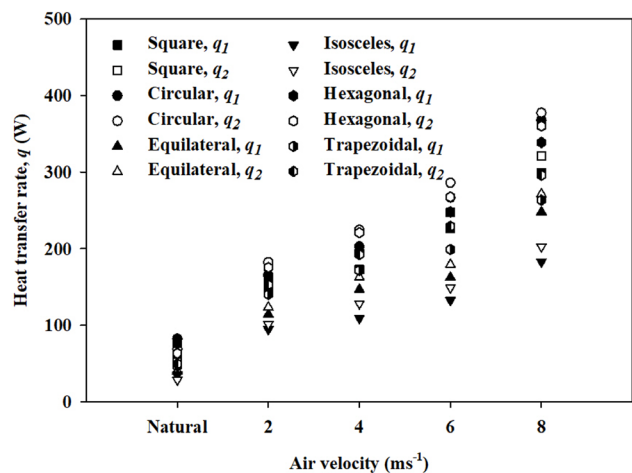


Fig. 13 Nusselt number, Nu for different geometrical shapes on multiple air velocity



(a)



(b)

Fig. 14 Forced convective heat transfer performance of different geometrical shapes (a) heat transfer coefficient, h ($W/m^2 \text{ } ^\circ C$), (b) heat transfer rate, q (W)

According to the literature, the triangular-shaped ribs have the maximum heat transfer coefficient among square, triangular, circular, and semi-circular ribs [42]. Promvonge and Thianpong [47] studied the thermal performance assessment of forced convection heat transfer for different shaped ribs such as triangular (isosceles), wedge (right triangular), and rectangular shapes for Reynolds numbers ranging from 4.000 to 16.000 in a rectangular channel where the triangular rib shows higher thermal performance.

In the present study, it is also found that the heat transfer coefficient is higher for triangular shapes than for other geometrical shapes. As shown in Fig. 14 (a), the heat transfer coefficient, h is higher for the isosceles shape than any other shape in this present study for forced convective heat transfer. The trapezoidal has a lower h than the equilateral but higher than the hexagonal shape and the circular has the lowest value. In addition, Fig. 14 (b) represents the heat transfer rate, q (W) for convective heat transfer, and it is visible that the circular one has the highest rate of heat transfer, whereas the isosceles has the lowest heat transfer rate.

4.3 Performance comparison between natural and forced convection

All the calculated characteristics for both the natural and forced convective heat transfer are plotted against the geometrical shapes. Fig. 15 shows the Nu , h and q to have a better view of the influence of the geometrical shape on heat transfer. The Nu , h and q are the lowest for the natural convective heat transfer, however, these values are increased with the increase the fluid velocity i.e. for the forced convective heat transfer. Interestingly, Nu is higher for circular shape than any other geometries and h is

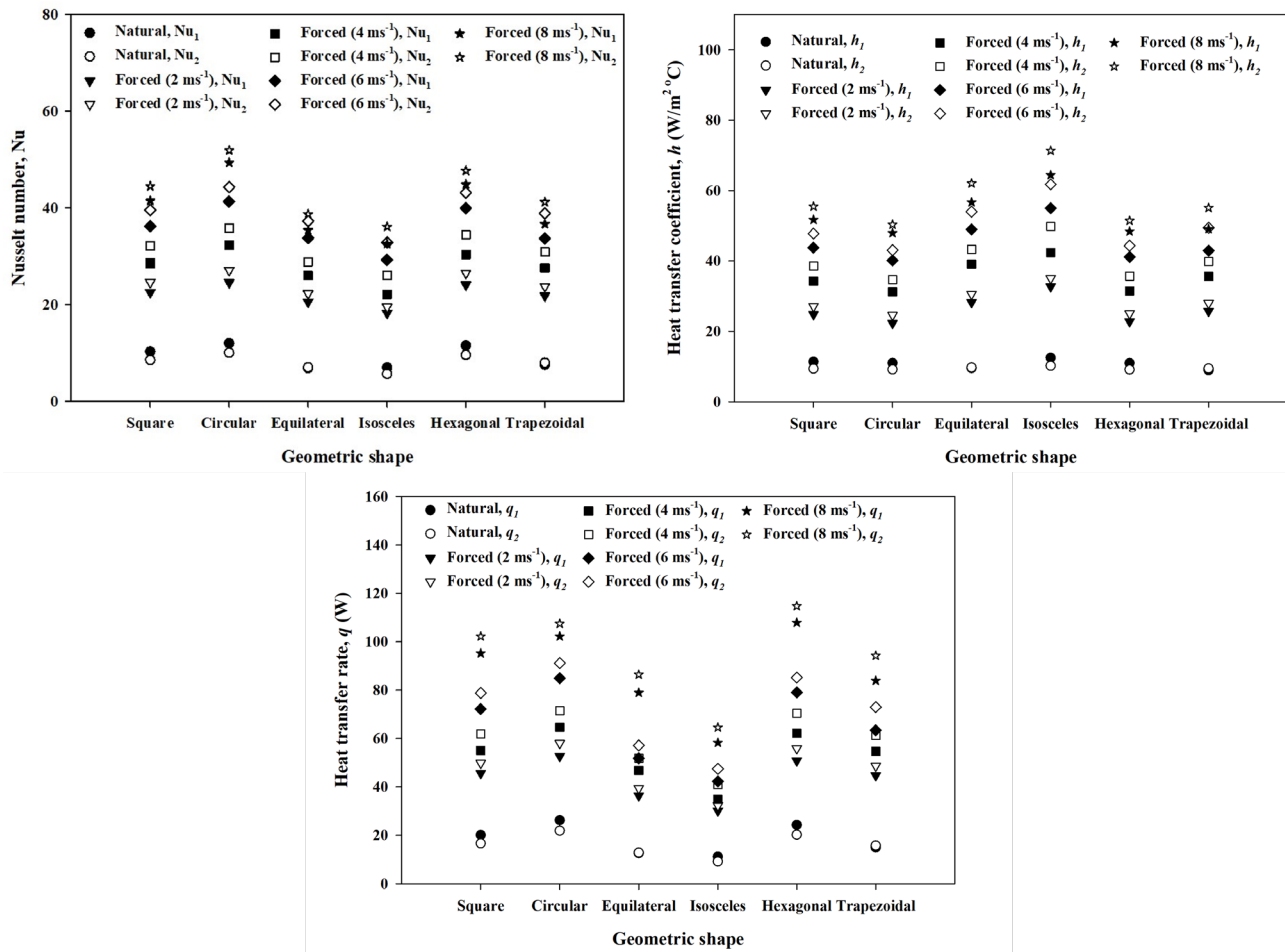


Fig. 15 Comparison of Nu , h and q for different geometrical shape for both natural and forced convection heat transfer

higher for isosceles shape than any other geometries. Similarly, Nu is found lowest for isosceles and h is found lowest for circular shape. With the consistency of the Nu , the heat transfer rate q shows higher and lower for circular and isosceles cylinder respectively.

In the present experimental study, the perimeter of all the geometrical shapes are kept constant to investigate the heat transfer characteristics for both natural and forced convective heat transfer. Based on the perimeter and cross-sectional area, the hydraulic diameter is lowest for isosceles and maximum for circular shape geometry. Therefore, the results obtained from the experimental study indicate that the heat transfer rate is basically influenced by the hydraulic diameter of the given geometrical shape. In addition, Nu follows the same trend and h follows the opposite trend as Nu is the product of the h and characteristics length or hydraulic diameter and inverse of the constant thermal conductivity. Indeed, the h is much influenced by the hydraulic diameter for the different geometrical shapes.

The results obtained from the experimental study also reveal that the heat transfer and its relevant characteristics are greatly influenced by the geometrical shape. Even though the perimeters of all the specimens are the same, the hydraulic diameter and in fact, the cross-sectional area is varied. Based on the geometrical shape and dimensions, the isosceles has the lowest hydraulic diameter and cross-sectional area whereas the circular shape has the maximum values of hydraulic diameter and hence the cross-sectional area. Interestingly, the Nu and q are exactly reflected based on hydraulic diameter or cross-sectional area for the different geometrical shapes. Even though the surface area is commonly emphasized as one of the influencing parameters to enhance heat transfer, cross-sectional area inherently plays a major role. In the present study, the lateral surface area is considered to calculate the heat transfer rate. It should be noted here that the two sides of each bar are around 6% of the total surface area of the specimen which is excluded in the heat transfer calculation. Therefore, it is obtained from the study that

cross sectional areas make significant contributions to the heat transfer even though the perimeter and lateral surface are the same for all the geometrical shapes.

It is also interesting that the heat transfer coefficient, h shows an opposite trend of geometrical shapes as compared with the heat transfer rate, q . In principle, q is proportional to h as per Newton's cooling law. However, in the present study, a significant contribution comes from the temperature on the surface of the metal bar. During the heating process of the metal bars in the present study, natural cooling also took place. That means for all cases, the surface temperatures are not the same and this is much more varied for the geometrical shapes. In this context, the temperature profiles during heating or cooling Figs. 6 and 7 reveal that isosceles takes the shortest time and the hexagonal shape takes the longest time to attain the steady state conditions. Moreover, the circular shape attained the highest temperature at steady state conditions and the hexagonal was next closest to the circular shape, however, the isosceles had the lowest temperature Fig. 6. In fact, among the six geometrical shapes, the isosceles shape is the most non-symmetry from the center to the edges. Therefore, the heat transfer from the center to the edges or surface for different locations varies and attains earlier in steady state conditions. On the other hand, the center to the edge is the largest for a hexagonal shape and eventually takes a longer time to have steady state condition. In fact, the heat transfer with the solid bars is mainly in the conductive mode which is influenced by the distance or the thickness as the heat propagates through the metal solid bar. Therefore, in terms of Nu and q , the effective geometrical shape would be circular, hexagonal, square, trapezoidal, equilateral, and isosceles. However, for the effective h values, the opposite sequence of the cross section of the geometrical shapes is obtained from the experimental studies for both the natural and forced convective heat transfer while the perimeters and the lateral surface area are kept constant for all the geometrical shapes.

References

- [1] Sharma, N., Tariq, A., Mishra, M. "Experimental Investigation of Heat Transfer Enhancement in Rectangular Duct with Pentagonal Ribs", *Heat Transfer Engineering*, 40(1–2), pp. 147–165, 2018. <https://doi.org/10.1080/01457632.2017.1421135>
- [2] Han, J. C., Park, J. S., Lei, C. K. "Heat Transfer Enhancement in Channels with Turbulence Promoters", *Journal of Engineering for Gas Turbines and Power*, 107(3), pp. 628–635, 1985. <https://doi.org/10.1115/1.3239782>
- [3] Chamoli, S., Thakur, N. S. "Thermal Behavior in Rectangular Channel Duct Fitted With V-Shaped Perforated Baffles", *Heat Transfer Engineering*, 36(5), pp. 471–479, 2014. <https://doi.org/10.1080/01457632.2014.935218>
- [4] Sa, K.-J., Afzal, A., Kim, K.-Y. "Performance Analysis and Design Optimization of Gapped Pin-Fin in a Cooling Channel", *Heat Transfer Engineering*, 39(6), pp. 549–567, 2017. <https://doi.org/10.1080/01457632.2017.1320170>

5 Conclusions

Experimental studies have been carried out to enhance the heat transfer rate with six different geometrical shapes of the metal bars, namely square, equilateral, isosceles, circular, hexagonal, and trapezoidal by keeping the same perimeter and length for all metal bars. The natural, as well as the forced convective heat transfer with four different air velocities, are considered for the experimental studies while the lateral surface area is considered for the necessary calculations. Experimental results reveal that the heat transfer characteristics are greatly influenced by the geometrical shape. Isosceles and circular shapes contribute to having the lowest and highest heat transfer rates respectively for both natural and forced convection. From the geometrical aspect, with the same perimeter, isosceles has the lowest cross sectional area and also the lowest hydraulic diameter, on other hand, circular shape has the highest cross sectional area and highest hydraulic diameter among the selected geometrical shapes. Therefore, even with the same perimeter, it is found that cross sectional area or the hydraulic diameter plays a major role in heat transfer characteristics. However, it is also revealed that the isosceles shape reaches the steady state quicker as compared with the other shapes while the hexagonal shape takes the longest time. This finding indicates that conductive heat transfer also plays a role in how the heat carries from the center of the bar to the all edges of the geometries. Therefore, the heat transfer characteristics are greatly influenced by the geometrical shape and the cross sectional area. A general correlation of the Nu and Re for different geometrical shapes with a wide range of Re for the forced convective heat transfer is also obtained.

Acknowledgement

This work was being supported by the Mechanical and Production Engineering Department (MPE) of Ahsanullah University of Science and Technology (AUST).

- [5] Acharya, S., Dutta, S., Myrum, T. A., Baker, R. S. "Periodically developed flow and heat transfer in a ribbed duct", *International Journal of Heat and Mass Transfer*, 36(8), pp. 2069–2082, 1993.
[https://doi.org/10.1016/s0017-9310\(05\)80138-3](https://doi.org/10.1016/s0017-9310(05)80138-3)
- [6] Tariq, A., Singh, K., Panigrahi, P. K. "Flow and Heat Transfer in a Rectangular Duct with Single Rib and Two Ribs Mounted on the Bottom Surface", *Journal of Enhanced Heat Transfer*, 10(2), pp. 171–198, 2003.
<https://doi.org/10.1615/jenhheattransf.v10.i2.50>
- [7] Rau, G., C, akan, M., Moeller, D., Arts, T. "The Effect of Periodic Ribs on the Local Aerodynamic and Heat Transfer Performance of a Straight Cooling Channel", *Journal of Turbomachinery*, 120(2), pp. 368–375, 1998.
<https://doi.org/10.1115/1.2841415>
- [8] Kumar, A., Bhagoria, J. L., Sarviya, R. M. "Heat transfer and friction correlations for artificially roughened solar air heater duct with discrete W-shaped ribs", *Energy Conversion and Management*, 50(8), pp. 2106–2117, 2009.
<https://doi.org/10.1016/j.enconman.2009.01.025>
- [9] Peng, W., Jiang, P.-X., Wang, Y.-P., Wei, B.-Y. "Experimental and numerical investigation of convection heat transfer in channels with different types of ribs", *Applied Thermal Engineering*, 31(14–15), pp. 2702–2708, 2011.
<https://doi.org/10.1016/j.applthermaleng.2011.04.040>
- [10] Manca, O., Nardini, S., Ricci, D. "Numerical investigation of air forced convection in channels with differently shaped transverse ribs", *International Journal of Numerical Methods for Heat & Fluid Flow*, 21(5), pp. 618–639, 2011.
<https://doi.org/10.1108/09615531111135864>
- [11] Rao, B. K. "Heat transfer to non-Newtonian flows over a cylinder in cross flow", *International Journal of Heat and Fluid Flow*, 21(6), pp. 693–700, 2000.
[https://doi.org/10.1016/s0142-727x\(00\)00063-1](https://doi.org/10.1016/s0142-727x(00)00063-1)
- [12] Holman, J. P., White, P. R. S. "Heat transfer", McGraw-Hill, 1992. ISBN 9780071126441
- [13] Bergman, T. L., Lavine, A. S., Incropera, F. P., DeWitt, D. P. "Fundamentals of heat and mass transfer", Wiley, 2018. ISBN 978-1-119-35388-1
- [14] Sak, C., Liu, R., Ting, D. S.-K., Rankin, G. W. "The role of turbulence length scale and turbulence intensity on forced convection from a heated horizontal circular cylinder", *Experimental Thermal and Fluid Science*, 31(4), pp. 279–289, 2007.
<https://doi.org/10.1016/j.expthermflusci.2006.04.007>
- [15] Bassam, A., Abu-Hijleh, K. "Laminar mixed convection correlations for an isothermal cylinder in cross flow at different angles of attack", *International Journal of Heat and Mass Transfer*, 42(8), pp. 1383–1388, 1999.
[https://doi.org/10.1016/s0017-9310\(98\)00249-x](https://doi.org/10.1016/s0017-9310(98)00249-x)
- [16] Bilen, K., Akyol, U., Yapici, S. "Heat transfer and friction correlations and thermal performance analysis for a finned surface", *Energy Conversion and Management*, 42(9), pp. 1071–1083, 2001.
[https://doi.org/10.1016/s0196-8904\(00\)00119-9](https://doi.org/10.1016/s0196-8904(00)00119-9)
- [17] Rong-Hua, Y. "An analytical study of the optimum dimensions of rectangular fins and cylindrical pin fins", *International Journal of Heat and Mass Transfer*, 40(15), pp. 3607–3615, 1997.
[https://doi.org/10.1016/s0017-9310\(97\)00010-0](https://doi.org/10.1016/s0017-9310(97)00010-0)
- [18] A/K Abu-Hijleh, B. "Enhanced Forced Convection Heat Transfer From a Cylinder Using Permeable Fins", *Journal of Heat Transfer*, 125(5), pp. 804–811, 2003.
<https://doi.org/10.1115/1.1599371>
- [19] Cebeci, T., Bradshaw, P. "Solution Manual and Computer Programs for Physical and Computational Aspects of Convective Heat Transfer", Springer New York, NY, 1988. ISBN 978-0-387-96825-4
<https://doi.org/10.1007/978-1-4612-3918-5>
- [20] Chang, S.-W., Wu, H.-W., Guo, D.-Y., Shi, J.-jie, Chen, T.-H. "Heat transfer enhancement of vertical dimpled fin array in natural convection", *International Journal of Heat and Mass Transfer*, 106, pp. 781–792, 2017.
<https://doi.org/10.1016/j.ijheatmasstransfer.2016.09.094>
- [21] Chu, W.-X., Lin, Y.-C., Chen, C.-Y., Wang, C.-C. "Experimental and numerical study on the performance of passive heat sink having alternating layout", *International Journal of Heat and Mass Transfer*, 135, pp. 822–836, 2019.
<https://doi.org/10.1016/j.ijheatmasstransfer.2019.02.034>
- [22] Adhikari, R. C., Wood, D. H., Pahlevani, M. "Optimizing rectangular fins for natural convection cooling using CFD", *Thermal Science and Engineering Progress*, 17(3), 100484, 2020.
<https://doi.org/10.1016/j.tsep.2020.100484>
- [23] Kadle, D. S., Sparrow, E. M. „Numerical and Experimental Study of Turbulent Heat Transfer and Fluid Flow in Longitudinal Fin Arrays", *ASME Journal of Heat and Mass Transfer*, 108(1), pp. 16–23, 1986.
<https://doi.org/10.1115/1.3246883>
- [24] Ayli, E., Bayer, O., Aradag, S. "Experimental investigation and CFD analysis of rectangular profile FINS in a square channel for forced convection regimes", *International Journal of Thermal Sciences*, 109, pp. 279–290, 2016.
<https://doi.org/10.1016/j.ijthermalsci.2016.06.021>
- [25] Adhikari, R. C., Wood, D. H., Pahlevani, M. "An experimental and numerical study of forced convection heat transfer from rectangular fins at low Reynolds numbers", *International Journal of Heat and Mass Transfer*, 163(14), 120418, 2020.
<https://doi.org/10.1016/j.ijheatmasstransfer.2020.120418>
- [26] Chen, H.-T., Lai, S.-T., Huang, L.-Y. "Investigation of heat transfer characteristics in plate-fin heat sink", *Applied Thermal Engineering*, 50(1), pp. 352–360, 2013.
<https://doi.org/10.1016/j.applthermaleng.2012.08.040>
- [27] Sun, R., Song, G., Zhang, D., Deng, J., Su, G. H., Kulacki, F. A., Tian, W., Qiu, S., "Experimental study of single-phase flow and heat transfer in rectangular channels under uniform and non-uniform heating", *Experimental Thermal and Fluid Science*, 114(8), 110055, 2020.
<https://doi.org/10.1016/j.expthermflusci.2020.110055>
- [28] VanFossen, G. J., "Heat-Transfer Coefficients for Staggered Arrays of Short Pin Fins", *Journal of Engineering for Power*, 104(2), pp. 268–274, 1982.
<https://doi.org/10.1115/1.3227275>
- [29] Morgan, V. T. "The The Overall Convective Heat Transfer from Smooth Circular Cylinders", *Advances in Heat Transfer*, 11, pp. 199–264, 1975.
[https://doi.org/10.1016/s0065-2717\(08\)70075-3](https://doi.org/10.1016/s0065-2717(08)70075-3)

- [30] Nakamura, H., Igarashi, T. "Variation of Nusselt number with flow regimes behind a circular cylinder for Reynolds numbers from 70 to 30000", *International Journal of Heat and Mass Transfer*, 47(23), pp. 5169–5173, 2004.
<https://doi.org/10.1016/j.ijheatmasstransfer.2004.05.034>
- [31] Hilpert, R. "Wärmeabgabe von geheizten Drähten und Röhren im Luftstrom", *Forschung auf dem Gebiete des Ingenieurwesens A*, 4(5), pp. 215–224, 1933.
<https://doi.org/10.1007/bf02719754>
- [32] Richardson, P. D. "Heat and mass transfer in turbulent separated flows", *Chemical Engineering Science*, 18(3), pp. 149–155, 1963.
[https://doi.org/10.1016/0009-2509\(63\)85001-0](https://doi.org/10.1016/0009-2509(63)85001-0)
- [33] Igarashi, T., Hirata, M. "Heat transfer in separated flows. II - Theoretical analysis", *Heat Transfer - Japanese Research*, 6(3), pp. 60–78, 1977.
- [34] Cieśliński, J. T., Smolen, S., Sawicka, D. "Free Convection Heat Transfer from Horizontal Cylinders", *Energies*, 14(3), 559, 2021.
<https://doi.org/10.3390/en14030559>
- [35] Kuehn, T. H., Goldstein, R. J. "Correlating equations for natural convection heat transfer between horizontal circular cylinders", *International Journal of Heat and Mass Transfer*, 19(10), pp. 1127–1134, 1976.
[https://doi.org/10.1016/0017-9310\(76\)90145-9](https://doi.org/10.1016/0017-9310(76)90145-9)
- [36] Kuehn, T. H., Goldstein, R. J. "Numerical solution to the Navier-stokes equations for laminar natural convection about a horizontal isothermal circular cylinder", *International Journal of Heat and Mass Transfer*, 23(7), pp. 971–979, 1980.
[https://doi.org/10.1016/0017-9310\(80\)90071-x](https://doi.org/10.1016/0017-9310(80)90071-x)
- [37] Kim, B. S., Lee, D. S., Ha, M. Y., Yoon, H. S. "A numerical study of natural convection in a square enclosure with a circular cylinder at different vertical locations", *International Journal of Heat and Mass Transfer*, 51(7–8), pp. 1888–1906, 2008.
<https://doi.org/10.1016/j.ijheatmasstransfer.2007.06.033>
- [38] Angeli, D., Pagano, A., Corticelli, M. A., Fichera, A., Barozzi, G. S. "Bifurcations of natural convection flows from an enclosed cylindrical heat source", *Frontiers in Heat and Mass Transfer*, 2(2), 2011.
<https://doi.org/10.5098/hmt.v2.2.3003>
- [39] Rath, S., Dash, M. K., Dash, S. K. "Natural convection from horizontal cylinders of different shapes in a rectangular enclosure", In: *Proceeding of Proceedings of the 24th National and 2nd International ISHMT-ASTFE Heat and Mass Transfer Conference (IHMTc-2017)*, BITS Pilani, Hyderabad, India 2018, pp. 1615–1620. ISBN 978-1-56700-478-6
<https://doi.org/10.1615/ihmtc-2017.2240>
- [40] Churchill, S. W., Usagi, R. "A general expression for the correlation of rates of transfer and other phenomena", *AIChE Journal*, 18(6), pp. 1121–1128, 1972.
<https://doi.org/10.1002/aic.690180606>
- [41] Churchill, S. W., Chu, H. H. S. "Correlating equations for laminar and turbulent free convection from a horizontal cylinder", *International Journal of Heat and Mass Transfer*, 18(9), pp. 1049–1053, 1975.
[https://doi.org/10.1016/0017-9310\(75\)90222-7](https://doi.org/10.1016/0017-9310(75)90222-7)
- [42] Ahn, S. W. "The effects of roughness types on friction factors and heat transfer in a roughened rectangular duct", *International Communications in Heat and Mass Transfer*, 28(7), pp. 933–942, 2001.
[https://doi.org/10.1016/s0735-1933\(01\)00297-4](https://doi.org/10.1016/s0735-1933(01)00297-4)
- [43] Wang, L., Sundén, B. "Experimental investigation of local heat transfer in a square duct with various-shaped ribs", *Heat and Mass Transfer*, 43(8), pp. 759–766, 2007.
<https://doi.org/10.1007/s00231-006-0190-y>
- [44] Diani, A., Mancin, S., Zilio, C., Rossetto, L. "An assessment on air forced convection on extended surfaces: Experimental results and numerical modeling", *International Journal of Thermal Sciences*, 67(1), pp. 120–134, 2013.
<https://doi.org/10.1016/j.ijthermalsci.2012.11.012>
- [45] Barik, A. K., Mukherjee, A., Patro, P. "Heat transfer enhancement from a small rectangular channel with different surface protrusions by a turbulent cross flow jet", *International Journal of Thermal Sciences*, 98, pp. 32–41, 2015.
<https://doi.org/10.1016/j.ijthermalsci.2015.07.003>
- [46] Vázquez, M. S., Rodríguez, W. V., Issa, R. "Effects of ridged walls on the heat transfer in a heated square duct", *International Journal of Heat and Mass Transfer*, 48(10), pp. 2050–2063, 2005.
<https://doi.org/10.1016/j.ijheatmasstransfer.2004.10.036>
- [47] Promvong, P., Thianpong, C. "Thermal performance assessment of turbulent channel flows over different shaped ribs", *International Communications in Heat and Mass Transfer*, 35(10), pp. 1327–1334, 2008.
<https://doi.org/10.1016/j.icheatmasstransfer.2008.07.016>
- [48] Knudsen, J. G., Katz, D. L. "Fluid Dynamics and Heat Transfer", McGraw-Hill, , 1958.
<https://doi.org/10.1002/aic.690050304>
- [49] Churchill, S. W., Bernstein, M. "A Correlating Equation for Forced Convection From Gases and Liquids to a Circular Cylinder in Crossflow", *Journal of Heat Transfer*, 99(2), pp. 300–306, 1977.
<https://doi.org/10.1115/1.3450685>
- [50] Douglas, M. J. M., Churchill, S. W. "Recorrelation of data for convective heat transfer between gases and single cylinders with large temperature differences", *Chemical Engineering Progress Symposium Series*, 52(18), pp. 23–28, 1956.
- [51] McAdams, W. H. "Heat transmission", McGraw-Hill, 1954.
- [52] Özişik, M. N. "Heat transfer: A Basic Approach", McGraw Hill, 1984. ISBN 0-07-Y66460-9